Fabrication and metrology of an electro-optic polymer light modulator based on waveguide-coupled surface plasmon resonance

J.-J. Chyou
C.-S. Chu
Z.-H. Shih
C.-Y. Lin
National Central University
Department of Mechanical Engineering
Chung-Li 320, Taiwan

S.-J. Chen, MEMBER SPIE
National Cheng Kung University
Department of Engineering Science
Tainan 701, Taiwan
E-mail: sheanjen@mail.ncku.edu.tw

C.-F. Shu
National Chiao Tung University
Department of Applied Chemistry
Hsin-Chu 300, Taiwan

Abstract. This study presents a novel high-efficiency electro-optic (EO) light modulator whose operation is based on the attenuated total reflection effect, in which the surface plasmon wave is excited by an incident waveguide light wave. The EO light modulator is fabricated using a nonlinear optical polymer material that is a side-chain EO polyimide with 2-[*N*-ethyl-4-(tricyanovinyl)anilino]ethanol chromophore. The modulator is characterized, and its performance tested, in terms of the thickness and dielectric constant of the polymer thin film, the EO coefficient, the insertion loss, and the modulation index. Additionally, the dynamic response of the EO light modulator is fully investigated and discussed.
 [DOI: 10.1117/1.1868775]

Subject terms: surface plasmon resonance; attenuated total reflection; electro-optic polymer; waveguide-coupled; nonlinear optical.

Paper 040172 received Mar. 29, 2004; revised manuscript received Aug. 18, 2004; accepted for publication Sep. 2, 2004; published online Mar. 10, 2005.

1 Introduction

The increasing demand in the optical communications field for light modulators with broader bandwidths and higher efficiency has led to the recent development of electro-optic (EO) light modulators, which provide a fast frequency response (>10 GHz) and avoid undesirable wavelength modulation by applying a direct current modulation of the laser diode.[1] EO materials are generally divided into two types, namely inorganic crystalline materials such as lithium niobate ($LiNbO_3$), silica, and GaAs, and organic polymer materials such as polymer and acrylic. Commercial EO modulators using inorganic crystalline materials are generally found in optical communication applications, which demand safe operation and extended life cycles. However, these devices not only are fragile and expensive, but also require a high modulation voltage and yield only a limited modulated spectrum. In contrast, organic EO materials such as nonlinear optical (NLO) polymers offer numerous advantages, including a straightforward manufacturing process, low cost, a wider frequency spectrum (>100 GHz), a low modulation voltage (<5 V), lower optical loss, and a high EO coefficient.[2] Since EO polymer materials are at least 10 times faster than their inorganic crystalline counterparts, and are cheaper and generally more suitable for the emerging high-frequency optical communications applications, many researchers have investigated their use in the design of EO light modulators.[3–6]

Many studies have investigated surface plasmon resonance (SPR) EO light modulators that utilize the attenuated total reflection (ATR) method.[3,5–9] SPR is an optical phenomenon in which an incident transverse magnetic (TM) light wave excites a surface plasmon wave (SPW) existing along the interface between a thin metal film and a dielectric medium. When the phase conditions of the two waves at the interface match, the majority of the incident light energy is transferred into the SPW and subsequently generates the ATR spectrum.[10] The high sensitivity of the propagation constant to the interfacial properties of the metal film and the dielectric sample medium renders SPR particularly suitable for biosensors[11] and light modulators.[3,5–6]

The SPR light modulator can provide lower optical loss, easier alignment, and a lower modulation voltage requirement.[4,5] A high-frequency SPR EO light modulator using a piezoelectric material has been proposed, but requires a high modulation voltage.[7] An EO light modulator utilizing an EO thin film has also been proposed.[8] This modulator electrically enhances the efficiency of the collimating monochromatic beam coupling into a long-range SPR (LRSPR), thereby reducing the required modulating voltage. A high-frequency SPR modulator (≈22 GHz) using an inorganic EO material (GaAs) has been fabricated, but has a low modulation index (0.1%).[9] Although the modulation index of EO light modulators employing EO thin films has been improved by electrically varying the efficiency of the coupling of a collimating monochromatic beam into the SPW, the modulation voltage at these voltages may be as high as 100 V.[3] An EO polymer light modulator with a waveguide structure, in which the efficiency of the waveguide-coupled resonance (WCR) is varied electrically, has also been presented.[5] To enhance the modulation efficiency of EO light modulators, the present study proposes a novel design that electrically varies the degree of coupling of the collimating monochromatic beam into the waveguide-coupled surface plasmon resonance (WCSPR). It is shown that this device is far more efficient than either the SPR, the LRSPR, or the WCR EO light modulator.

In this paper, we report some of our work on fabricating, characterizing, and testing an EO polymer modulator made

0091-3286/2005/$22.00

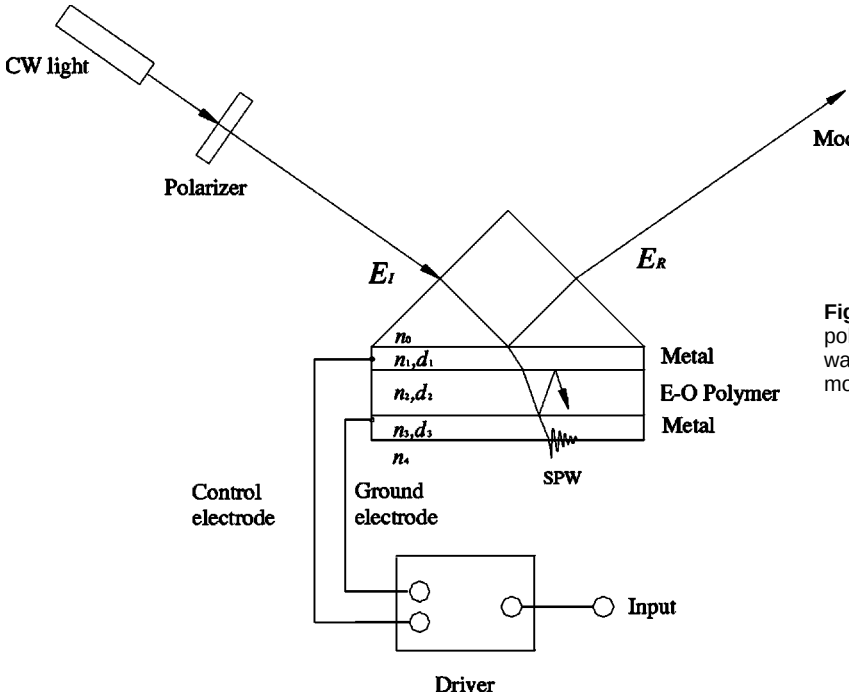

Fig. 1 Schematic layout of EO polymer light modulator with waveguide-coupled surface plasmon resonance.

from a side-chain EO polyimide with 2-[*N*-ethyl-4-(tricyanovinyl)anilino]ethanol chromophore.[12,13] Initially, we introduce the principles of the WCSPR light modulator, and then describes the fabrication of the proposed device, including the EO polymer preparation, the EO thin-film fabrication, and the poling process. The metrology of the modulator's performance is also discussed in terms of the EO coefficient, modulation index, stability, and radio-frequency (rf) modulation. Also, the dynamic response of the EO light modulator is fully investigated and discussed. Finally, we present some brief conclusions.

2 Waveguide-Coupled Surface Plasmon Resonance

The reflectivity of ATR light modulators is highly sensitive to the refractive index modulation of the EO thin film and to the slope at the working point chosen for the proposed modulation, within the dip of the SPR spectrum. To improve the efficiency of these modulators, this paper proposes a five-layered light modulator based on a modified Kretschmann ATR configuration. As shown in Fig. 1, the device consists of a control layer comprising a glass slide and a metal thin film, an EO polymer film waveguide layer, a metal thin-film ground electrode, and an air layer. Usually, Au or Ag is the best candidate for the metal thin films in the visible light region. The glass slide is optically contacted with a prism via an index-matching oil, which reduces the refractive index jump at the interface. In the angular interrogation mode, the incident TM light beam is partly reflected and partly transmitted when the incident angle is less than the critical angle at the interface between metal layer and prism. If the thickness of EO polymer is larger than half the wavelength of the incident TM light beam and satisfies a phase-matching condition for constructive interference inside the waveguide layer, the transmitted light beam will excite a surface plasmon wave along the interface between the gold ground electrode and the air layer. As shown in the figure, the waveguide layer results in multiple-beam Fabry-Perot (FP) interference. The excitation of the SPW at the interface between the gold ground electrode and the air buffer is influenced by the FP effect in the waveguide layer.

For the five-layered ATR coupling scheme shown in Fig. 1, the total reflection from the complex interface between n_0 and n_1 can be expressed as[6]

$$I=\frac{\dfrac{(|r_{01}|+|r_{1234}|)^2}{(1+|r_{01}|\cdot|r_{1234}|)^2}-F_{01234}\sin^2\left[\dfrac{\phi_{01}-(\phi_{1234}+\delta_1)}{2}\right]}{1-F_{01234}\sin^2\left[\dfrac{\phi_{01}+(\phi_{1234}+\delta_1)}{2}\right]}, \tag{1}$$

where $\delta_1=(4\pi/\lambda)n_1d_1\cos\theta_{t1}$ is the optical path difference induced by a metal layer (n_1) of thickness d_1, λ is the wavelength of the incident light, θ_{t1} is the angle of transmission at the interface between medium n_0 and n_1, ϕ_{ij} is the phase of the reflectivity r_{ij} from interface i to j, ϕ_{ijkl} is the phase of the reflectivity r_{ijkl} from interface i to l, and $F_{01234}=4|r_{01}|\cdot|r_{1234}|/(1+|r_{01}|\cdot|r_{1234}|)^2$ is the equivalent finesse coefficient of the FP interference.

The minimum value of the total reflection I in Eq. (1) occurs when the following relationship is satisfied:

$$\phi_{21}+\phi_{234}+\delta_2=2m\pi, \quad m=0,1,2,..., \tag{2}$$

where $\delta_2=(4\pi/\lambda)n_2d_2\cos\theta_{t2}$ is the optical path difference induced by the waveguide layer (n_2) of thickness d_2, and θ_{t2} is the transmission angle at the interface between media n_1 and n_2. Equation (2) describes the phase-matching condition of WCSPR, in which the majority of

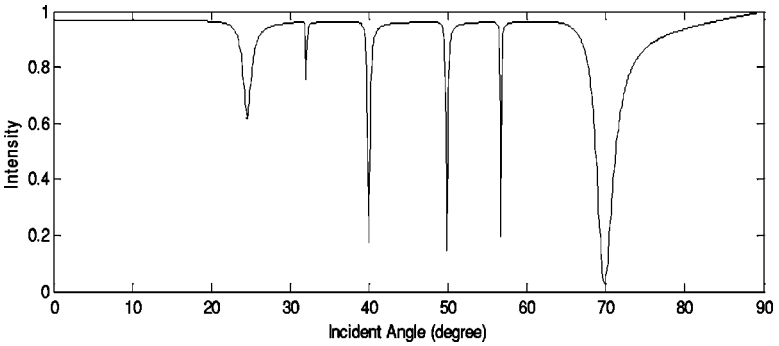

Fig. 2 Resonance angular positions for five-layered system [$\lambda=632.8$ nm; SF-59 prism ($n=1.964$), thin silver film ($e=-17.6+i0.67$, $d=30$ nm), EO polymer ($n=1.69$, $d=1000$ nm), silver ground electrode ($e=-17.6+i0.67$, $d=25$ nm)]. WCR: 24.5, 40, 48.2, and 56.7 deg; SPR: 70 deg; WCSPR: 32 deg.

the incident light photon energy transferred in the normal propagation mode in the waveguide layer is confined within the waveguide layer and is coupled with the SPW at the interface between the gold ground electrode and the air buffer. This coupling is indicated by a dip in the APR spectrum.

This reflectivity dip, with a 632.8-nm-wavelength light source, is observed as SPR, WCR, and WCSPR modes in the ATR spectrum shown in Fig. 2, where the various dips are calculated using the Fresnel equations [$\lambda=632.8$ nm; SF-59 prism ($n=1.964$), thin silver film ($e=-17.6+i0.67$, $d=30$ nm), EO polymer ($n=1.69$, $d=1000$ nm), silver ground electrode ($e=-17.6+i0.67$, $d=25$ nm)]. Besides the usual SPR dip located at an incident angle of 70 deg, a dip with a much steeper slope is evident at an incident angle of 32 deg. This dip is associated with the WCSPR resonance mode. The four remaining dips are all WCR mode resonances, for their positions coincide with the position matched with the waveguide mode. Moreover, the WCR dip at 24.5 deg is broader than the other WCR dips because its incident angle is less than the critical angle at the interface between prism and metal layer, so that the FP effect occurring in the waveguide layer is less enhanced.

To delineate the WCSPR phenomenon more clearly, the magnitude of the electric field distribution along the direction perpendicular to the film interface, E_z, is calculated theoretically for the WCSPR mode when the angular position of the incident light beam is fixed at 32 deg. The corresponding results, presented in Fig. 3, indicate that the multiple beam reflection inside the waveguide layer couples with the SPW at the interface between the metal electrode and the air if the thickness and refraction index of the waveguide layer satisfy the phase-matching condition. Under these conditions, the electric field is significantly enhanced. In other words, the magnitude of the electric field is much stronger at the interface than within the waveguide when the incidence angle corresponds to the WCSPR angular position. Figure 2 demonstrates that the reflectivity dip in the WCSPR mode is much narrower than the dips associated with the traditional SPR or WCR spectrums. Consequently, the optimal working angle of the modulator is specified to be close to the resonance angle of the WCSPR mode rather than to the angle of either the SPR or WCR modes. Subsequently, this study adopted the proposed WCSPR mode as the optimal design for a light modulator.

The modulation relationship between the EO coefficient of the EO polymer and the applied voltage is given by[9]

$$\frac{\Delta R}{\Delta V}=-n_2^3\frac{r_{33}}{\lambda}\frac{\pi}{4\Gamma_i d_2}, \tag{3}$$

where ΔR is reflectance change due to the applied voltage ΔV, n_2 is the refractive index of the EO polymer material before modulation, r_{33} is the EO coefficient of the EO polymer, d_2 is the thickness of the EO thin film, λ is the wavelength of the incident light, and Γ_i is the internal damping of the light modulator. From Eq. (3), the EO modulator becomes more efficient as the applied voltage decreases and the resulting reflectance change increases. Therefore, in view of the superior EO coefficients of EO polymer and the greater sensitivity to reflectance change of the WCSPR than of other modes, we choose the WCSPR dip as the working position for the modulator.

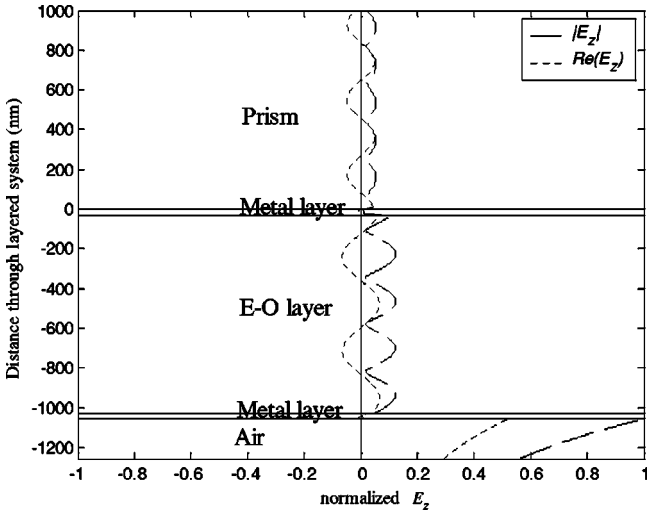

Fig. 3 Magnitude of electric field distribution along the direction perpendicular to the film interface (E_z) at an incident angle of 32 deg.

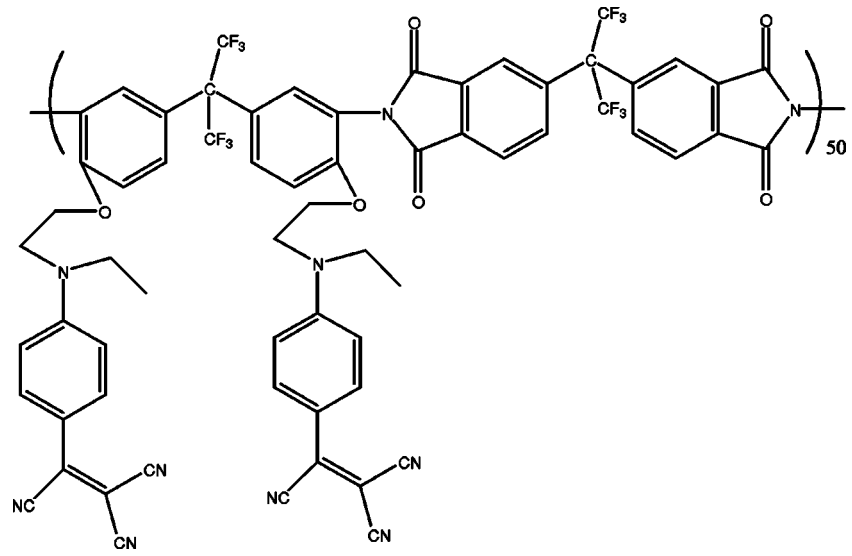

Fig. 4 The side-chain EO polyimide with 2-[*N*-ethyl-4-(tricyanovinyl)anilino]ethanol chromophore.

3 Fabrication

3.1 *EO Polymer Thin-Film Fabrication*

Since the modulation efficiency is closely related to the properties of the EO thin film, the selection of an appropriate EO material for the waveguide is crucial. This study employs the NLO side-chain EO polyimide with 2-[*N*-ethyl-4-(tricyanovinyl)anilino]ethanol chromophore, shown in Fig. 4, as the EO waveguide material.[12,13] The properties of this EO polymer include: (a) a glass transition temperature of approximately 183°C, (b) a maximum wavelength absorption of approximately 520 nm, (c) a high solubility, which enhances film formation, and (d) good thermal stability, which permits 90% EO coefficient retention after 400 h in a 100°C environment.[12] The EO polymer used was prepared by using a solvent such as cyclohexanone or chloroform to dissolve 15 wt% of NLO polymer solid powder. The resulting polymer solution was then sifted through a 0.2-μm filter.[13]

In fabricating the EO polymer modulator, a continuous deposition system (ARC-12M, Plasma Science Co.) was used to sputter-coat a gold film onto the glass slide (BK-7, $n_0 = 1.515$) in order to form the control electrode. The thickness of the gold film was controlled to be 30 nm (area 19.634 mm^2) with an accuracy of 1 nm. Subsequently, the EO polymer waveguide layer, made of NLO side-chain E-O polyimide, was spin-coated onto the substrate using a spinning machine (K-359SD-1 by Kyowariken Co.). In the spinning process, 0.01 ml of the polymer solution was used and the machine was operated at 1000 rpm for 30 s. The thickness of the EO polymer waveguide film was controlled to be approximately 1 μm. Using an atomic force microscope (AFM), the surface roughness of the EO polymer was observed to be approximately 1.1 nm. The samples were baked in a vacuum oven at 145°C for a minimum of 12 h and then placed on the top of the hot stage at 160°C for 30 min in order to remove the solvent. Finally, a gold film was sputter-coated onto the samples to form the ground electrode for the poling and modulation processes. The thickness of the gold electrode was controlled at approximately 35 nm (area 7.08 mm^2), and the overlapped modulation area was approximately 6.25 mm^2.

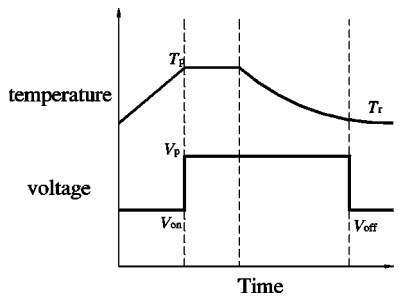

Fig. 5 Contact poling process for EO polymer. T_p: poling temperature; T_r: room temperature; V_p: poling voltage.

3.2 *Poling Process*

A contact poling process was applied to the EO polymer modulator to align the nonlinear molecular structure of the EO polymer.[14] In this process, an 80-V/μm dc electric field was applied for 20 min in a 150°C environment, and the polymer was then allowed to cool to room temperature while the electric field was maintained at the poling voltage. The temperature-time chart for this contact poling process is shown in Fig. 5. The strong dipole moment orients the NLO polymers, causing the EO polymer to become noncentrosymmetric and the EO property to be enhanced. As shown in Table 1, the poling results, and hence the EO properties (such as the EO coefficient), are dependent on the poling process conditions: the temperature, voltage, and poling time. The results indicate that there is no change in the EO coefficient r_{33} if the poling time is less than 10 min and the poling temperature exceeds the glass transition temperature. The optimal EO coefficient is 6 pm/V, achieved with poling conditions of 170°C and 80 V/μm.

Table 1 EO properties for various poling conditions.

Poling time (min)	Poling temp. (°C)	Poling field (V/μm)	EO coeff. (pm/V)
5	170	90	0.87
5	175	95	0.87
10	170	80	6
20	170	80	6
20	150	80	6
20	175	80	6

4 Metrology

4.1 *Determination of Polymer Film Dielectric Constant and Thickness*

It is crucial that the optical properties of each layer within the modulator system be precisely predicted and monitored if the performance of the device is to be optimized. For instance, the original refractive index and thickness of the EO waveguide must be predicted before the modulating electric field across the EO thin film can be calculated from Eq. (3). Therefore, this study employs a home-made metrology system (see Fig. 1) to characterize the respective refractive indexes and thicknesses of the EO waveguide and metal layer. Several ATR-related techniques have been proposed previously to determine the optical properties (viz., the thickness *d* and relative permittivity *e*) of metal or dielectric thin films. These methods include: (a) a data-fitting technique that adjusts the parameters for optical properties until the theoretical plot obtained from the Fresnel equation closely approximates the experimental SPR spectrum,[15] (b) measuring angle-modulated spectra with two different buffers,[16] with two different wavelengths,[17] or with different metal thicknesses, (c) measuring wavelength-modulated spectra with two different incident angles,[18] and (d) data estimation based on linear statistical model analysis.[19,20]

The use of the data-fitting technique to determine the optical properties usually yields an ambiguous result. To circumvent this ambiguity, different wavelengths and a least-squares fit of the reflectance minimum at the resonant excitation of the SPW can be used to determine a unique correct solution.[21] In a previous study, the present authors devised an improved numerical analysis method, which combined modified linear data estimation and the multiexperiment linear data analysis method.[22] The latter method yields a more accurate solution for the parameters of interest than conventional analytical methods, reduces variability, and excludes the colored noise arising from accidental error noise incurred during the metrology process. Although the optical properties of the metal layer and gold electrode in the present modulator can be estimated using the multiexperiment data analysis method, it is difficult to predict the optical properties of the EO polymer from a single ATR spectrum, due to the virtual absence of the EO polymer absorption coefficient.

Since the ATR spectrum of an EO polymer light modulator system has many reflection dips, the present study devises an optical properties determination method which uses data fitting around two WCR dips located at different angular positions on a single ATR spectrum. This method is referred to as the two-waveguide-coupled-mode (TWCM) method, and is applicable to any ATR structure incorporating an EO waveguide of sufficient thickness to yield the WCR mode in its ATR spectrum. This method enables the estimation of the EO polymer optical properties either by solving the intersection of the possible solution curves in data fitting with two dips from two TE modes, or two TM modes, or one TE mode and one TM mode when the waveguide material is isotropic; or with two dips from two TE modes or two TM modes when the waveguide material is anisotropic (see Fig. 6). A data analysis of the present ATR spectrum reveals the following optical properties of the gold ground electrode: $n_3=0.266$, $k_3=3.520$, and $d_3=27.146$ nm. Meanwhile, TWCM analysis (Fig. 6) of the ATR spectrum (Fig. 7) shows that the optical properties of the EO thin film are $n_2=1.63$, $k_2=0.002$, and $d_2=1313$ nm. Similarly, data analysis indicates that the optical properties of the control gold electrode are $n_1=0.184$, $k_1=3.569$, and $d_1=35.026$ nm. The polymer film sample is then contacted with a prism to form the EO light modulator shown in Fig. 1. We use gold rather than silver in our proposed modulator for experiment because gold is more stable in the fabrication process. We also employed a BK-7 prism instead of an SF-59 prism because the BK-7 prism is cheap and easy to acquire. The working point of the EO light modulator is then specified as an incident angle of 36 deg. By calculating the magnitude of the electric field distribution E_z along the direction perpendicular to the film interface at $\theta=36$ deg, it is determined that the incident energy is totally confined within the waveguide EO layer and the SPW. In other words, the modulator is more efficient when the light wave is incident at this angle than at any other angular position.

4.2 *EO Coefficient*

To test the modulation performance of the proposed EO light modulator, a 30-V dc voltage was applied. The maximum reflection light modulation was found to be approximately 1.1%. The corresponding refractive index change was 0.00045. From Eq. (3), it was determined that the EO coefficient r_{33} of the EO thin film was about 9.8 pm/V. When the working point was specified as an incident angle of $\theta=36.2$ deg (WCSPR) and a 30-V dc voltage was applied, the insertion loss was measured as -3.4 dB. After poling, the EO film was found to remain stable for at least two months.

4.3 *Dynamic Response*

To perform dynamic modulation, a 10-MHz 7-V sine wave was applied across the EO polymer light modulator. The experimental results, presented in Fig. 8, indicate that the modulation index was equal to 0.5%, which is clearly less than the 4% value predicted theoretically. This unexpected performance might be attributed to the fact that the present experiment does not involve an optimal design condition, viz., the metal layer is gold rather than silver. Gold was used for the modulation experiment because of its stability in the fabrication process. Therefore, the modulation performance cannot be expected to be as good as the simulation result with silver film. By simulation with various

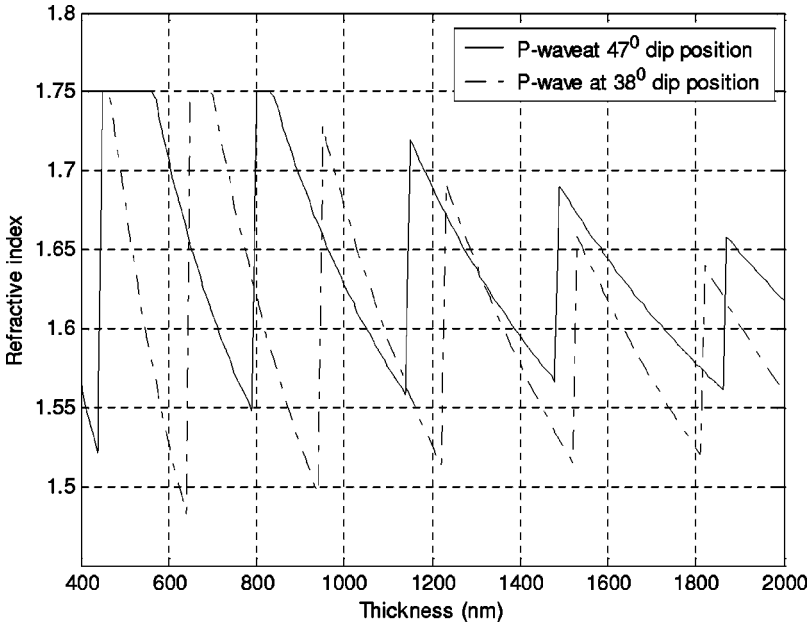

Fig. 6 Solutions for EO polymer by TWCM. (The optical properties of the EO thin film from the analysis are $n_2=1.63$, $k_2=0.002$, and $d_2=1313$ nm.)

noble metals, it is found that the SPR dip with silver film in the visible light region is the narrowest and sharpest. Therefore, silver is a better candidate for metal film in the visible region if the fabrication and stability can be controlled.[11] Furthermore, the modulator is not as fast as the theoretical bandwidth of 25 MHz, since the electrode area (active area 6.25 mm^2) is somewhat larger than the value used in the theoretical calculation (1 mm^2). If the fabrication process of the EO polymer light modulator can be further improved so that the ground electrode area is reduced, the bandwidth of the proposed EO polymer light modulator can be broadened correspondingly.

5 Conclusions

This study has fabricated, characterized, and tested an EO polymer light modulator. The modulation index, EO coefficient, and insertion loss in a 632.8-nm-wavelength free-space laser communication link have all been presented. The EO polymer fabrication process is straightforward, and hence the proposed modulator is suitable for mass production and for integration with semiconductor processes. The present study has demonstrated that the modulation efficiency can be improved by specifying an appropriate poling condition and by using the WCSPR mode as the working point.

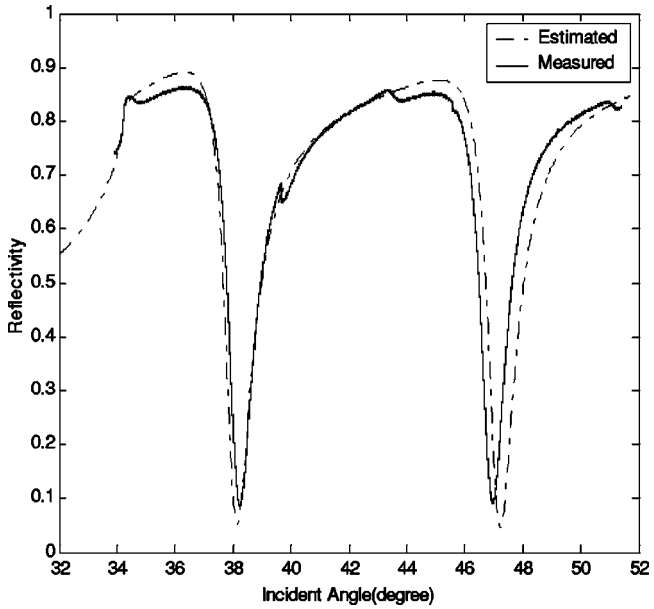

Fig. 7 ATR spectrum for prism (BK-7), gold film, and EO polymer.

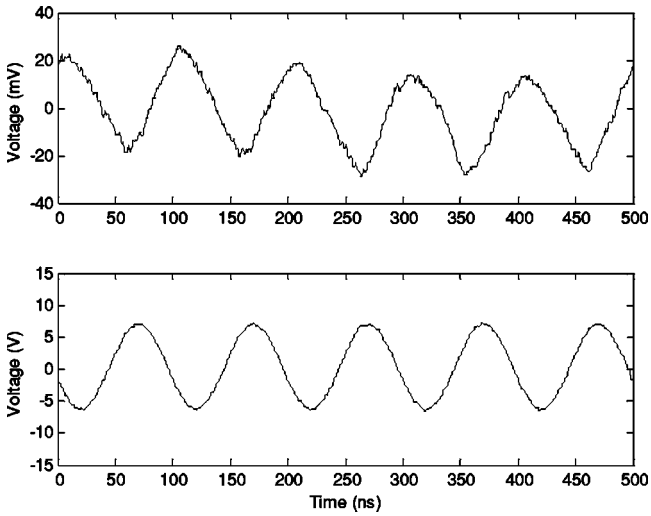

Fig. 8 Rf modulation on applying 14-V ac across the EO thin film: (a) output signal, (b) input signal.

Acknowledgments

The authors gratefully acknowledge the financial support provided to this study by the Taiwan Ministry of Education under grant No. A-91-E-FA08-1-4.

References

1. J. M. Senior, *Optical Fiber Communications: Principles and Practices*, 2nd ed., Prentice-Hall, New York (1992).
2. S.-S. Sun, S. Maaref, E. Alam, Y. Wang, Z. Fan, M. Bahoura, P. Higgins, and C. E. Bonner, ''Recent development of crosslinked NLO polymers for large bandwidth electro-optical modulations,'' *Proc. SPIE* **4580**, 297–308 (2001).
3. C. Jung, S. Yee, and K. Kuhn, ''Electro-optic polymer light modulator based on surface plasmon resonance,'' *Appl. Opt.* **34**(6), 946–949 (1995).
4. W. Wang, Y. Shi, D. J. Olson, W. Lin, and J. H. Bechtel, ''Push-pull poled polymer Mach-Zehnder modulators with a single microstrip line electrode,'' *IEEE Photonics Technol. Lett.* **11**, 51–53 (1999).
5. Y. Jiang, Z. Cao, G. Chen, X. Dou, and Y. Chen, ''Low voltage electro-optic polymer light modulator using attenuated total internal reflection,'' *Opt. Laser Technol.* **33**, 417–420 (2001).
6. J. Chyou, S.-J. Chen, C. Chu, Z. Shih, C. Lin, and K. Huang, ''High efficiency electro-optic polymer light modulator based on waveguide-coupled surface plasmon resonance,'' *Proc. SPIE* **5221**, 197–206 (2003).
7. G. T. Sincerbox and J. C. Gordon II, ''Small fast large-aperture light modulator using attenuated total reflection,'' *Appl. Opt.* **20**, 1491–1494 (1981).
8. J. Schildkraut, ''Long-range surface plasmon EO modulator,'' *Appl. Opt.* **27**, 4587–4590 (1988).
9. O. Solgaard, F. Ho, J. I. Thackara, and D. M. Bloom, ''High frequency attenuated total internal reflection light modulator,'' *Appl. Phys. Lett.* **61**(21), 2500–2502 (1992).
10. H. Raether, *Surface Plasmons on Smooth and Rough Surfaces and on Gratings*, Springer-Verlag, Berlin, Heidelberg (1988).
11. J. Homola, S. S. Yee, and G. Gauglitz, ''Surface plasmon resonance sensors: review,'' *Sens. Actuators B* **54**, 3–15 (1999).
12. T.-A. Chen, A. K.-Y. Jen, and Y. Cai, ''Facile approach to nonlinear optical side-chain aromatic polyimides with large second-order nonlinearity and thermal stability,'' *J. Am. Chem. Soc.* **117**, 7295–7296 (1995).
13. T.-A. Chen, A. K.-Y. Jen, and Y. Cai, ''Two-step synthesis of side-chain aromatic polyimides for second-order nonlinear optics,'' *Macromolecules* **29**, 535–539 (1996).
14. X. Zhang, X. Lu, L. Wu, and R. T. Chen, ''Contact poling of the nonlinear optical film for polymer-based electro-optic modulator,'' *Proc. SPIE* **4653**, 87–95 (2002).
15. J. M. Phelps and D. M. Taylor, ''Determining the relative permittivity and thickness of a lossless dielectric overlayer on a metal film using optically excited surface plasmon polaritons,'' *J. Phys. D* **29**, 1080–1087 (1996).
16. H. E. de Bruijn, B. S. F. Altenburg, R. P. H. Kooyman, and J. Greve, ''Determination of the thickness and dielectric constant of thin transparent dielectric layers using surface plasmon resonance,'' *Opt. Commun.* **82**, 425–432 (1991).
17. K. A. Peterlinz and R. Georgiadis, ''Two-color approach for determination thickness and dielectric constant of thin films using surface plasmon resonance spectroscopy,'' *Opt. Commun.* **130**, 260–266 (1996).
18. K. S. Johnston, S. R. Karlsen, C. C. Jung, and S. S. Yee, ''New analytical technique for characterization of thin films using surface plasmon resonance,'' *Math. Chem. Phys.* **42**, 242–246 (1995).
19. T. M. Chinowsky and S. S. Yee, ''Quantifying the information content of surface plasmon resonance reflection spectra,'' *Sens. Actuators B* **51**, 321–330 (1998).
20. T. M. Chinowsky, L. S. Jung, and S. S. Yee, ''Optimal linear data analysis for surface plasmon resonance biosensors,'' *Sens. Actuators B* **54**, 89–97 (1999).
21. W. P. Chen and J. M. Chen, ''Use of surface plasma waves for determination of the thickness and optical constants of thin metallic films,'' *J. Opt. Soc. Am.* **71**, 189–191 (1981).
22. J.-J. Chyou, S.-J. Chen, C.-S. Chu, C.-H. Tsai, F.-C. Chien, G.-Y. Lin, K.-T. Huang, W.-C. Ku, S.-K. Chiu, and C.-M. Tzeng, ''Multi-experiment linear data analysis for ATR biosensors,'' *Proc. SPIE* **4819**, 175–184 (2002).

S.-J. Chen received his BS degree from National Taiwan University in 1987 and MS degree in mechanical engineering from Columbia University in 1991. In December 1996, he was awarded a PhD degree for research in adaptive noise cancellation and image restoration at the University of California, Los Angeles (UCLA). He entered the Synchrotron Radiation Research Center in January 1998 to develop soft x-ray active gratings and microfocusing optical systems. He did most of his work in the field of adaptive optics and its applications. Currently, he is an assistant professor at National Cheng Kung University, and his principal research includes optical biosensors, adaptive optics, and optomechatronics.

Biographies and photographs of other authors not available.